INTERNATIONAL JOURNAL FOR NUMERICAL METHODS IN FLUIDS, VOL. 20, 1203–1213 (1995)

INTEGRAL TRANSFORM SOLUTION OF DEVELOPING LAMINAR DUCT FLOW IN NAVIER–STOKES FORMULATION*

J. S. PEREZ GUERRERO AND R. M. COTTA

Mechanical Engineering Department, EE/COPPE/UFRJ, Universidade Federal do Rio de Janeiro, Cidade Universitária, CP 68.503, Rio de Janeiro, RJ 21945.970, Brazil

SUMMARY

The generalized integral transform technique is employed in the hybrid numerical–analytical solution of the Navier–Stokes equations in streamfunction-only formulation, which govern the incompressible laminar flow of a Newtonian fluid within a parallel plate channel. Owing to the analytic nature of this approach, the outflow boundary condition for an infinite duct is handled exactly, and the error involved in considering finite duct lengths is investigated. The present error-controlled solutions are used to inspect the relative accuracy of previously reported purely numerical schemes and to compare Navier–Stokes and boundary layer formulations for various combinations of inlet conditions and Reynolds number.

KEY WORDS integral transforms; Navier–Stokes equations; channel flow; hybrid methods

INTRODUCTION

The analysis of low-Reynolds-number flows in channels is of vital importance in various branches of engineering sciences in connection with both heat and fluid flow applications. In such situations the simplifying assumptions in boundary layer theory may no longer be applicable and the full Navier–Stokes equations are required to model the physical problem. Explicit analytic solutions are not achievable even for laminar incompressible steady flow conditions, and numerical approaches for elliptic problems must be employed in the estimation of velocity and pressure fields along the hydrodynamic developing region of the channel. The numerical solution procedure is further complicated by the need to impose an outflow boundary condition for a finite duct length, which, if not appropriately chosen, may induce significant errors in the velocity field evaluations within the duct.

A literature review reveals an ongoing concern with the accurate solution of low-Reynolds-number flows inside channels. For the case of present interest, i.e. parallel plate channels, previously reported contributions[1–7] deal with different versions of the classical finite difference[1–5] and finite element [7] methods as well as with approximate analytic-type solutions obtained through linearization of inertia terms.[6] Various inlet flow conditions were considered, with particular emphasis on uniform parallel flow and, to a lesser extent, uniform irrotational inlet flow. The outflow boundary condition is in general handled via consideration of a fully developed velocity profile at a sufficiently large truncated duct length, established through successive numerical investigations. None of these approaches provides an accuracy-controlled numerical solution, and several computer runs are required to inspect

* Extended version of a paper presented at the 8th International Conference on Numerical Methods in Laminar and Turbulent Flow, Swansea, U.K., July 1993.

CCC 0271–2091/95/111203–11

Received 28 August 1992
Revised 31 August 1993

for the effects of mesh refinement and truncated domain extent on the final numerical results for the velocity field.

Recently, based on the ideas in the generalized integral transform technique (GITT),[8] a hybrid numerical–analytical approach for the incompressible steady state Navier–Stokes equations was advanced[9–11] and illustrated for the classical test problems of a lid-driven square cavity flow and natural convection within a porous cavity. The excellent convergence characteristics of the proposed eigenfunction expansion were demonstrated for various values of the governing parameters, and previously reported numerical solutions were validated in a more definitive way. The same success as in previous developments was achieved, including various non-linear diffusion and convection–diffusion problems [8] and the boundary layer equations for internal flow problems,[12–14] with automatic accuracy control.

The present work is aimed at further advancing the integral transform approach for the solution of the full Navier–Stokes equations in the context of internal flow applications. Numerical results with automatic error control are obtained for various values of the Reynolds number under both parallel and irrotational inlet flow conditions. The convergence behaviour of the proposed eigenfunction expansion is illustrated for some typical cases. Results for both inlet flow conditions are critically compared against each other and with the classical boundary layer formulation. Also, the effect of imposing a fully developed flow situation on a truncated finite duct length is inspected.

ANALYSIS

Two-dimensional steady incompressible laminar flow of a Newtonian fluid is considered, developing inside a parallel plate channel, with a uniform inlet longitudinal velocity distribution, for either parallel or irrotational flow (Figure 1). In dimensionless form and adopting the streamfunction-only formulation, the problem is given as

$$\nabla^4\psi(x, y) = \frac{Re}{4}P(x, y), \quad 0 < y < 1, \quad x > 0 \tag{1a}$$

where the streamfunction is defined in terms of the velocity components in the normal and longitudinal directions y and x respectively as

$$\frac{\partial\psi(x, y)}{\partial y} = u(x, y), \qquad \frac{\partial\psi(x, y)}{\partial x} = -v(x, y). \tag{1b,c}$$

The non-linear source term in equation (1a) is written as

$$P(x, y, \psi) = \frac{\partial\psi}{\partial y}\left(\frac{\partial^3\psi}{\partial x^3} + \frac{\partial^3\psi}{\partial y^2\partial x}\right) - \frac{\partial\psi}{\partial x}\left(\frac{\partial^3\psi}{\partial x^2\partial y} + \frac{\partial^3\psi}{\partial y^3}\right) \tag{1d}$$

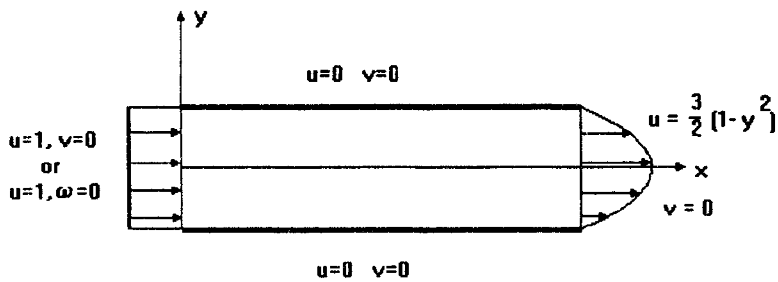

Figure 1. Geometry and co-ordinate system for developing duct flow

and the biharmonic operator is given by

$$\nabla^4 \equiv \frac{\partial^4}{\partial x^4} + 2\,\frac{\partial^4}{\partial x^2 \partial y^2} + \frac{\partial^4}{\partial y^4}. \tag{1e}$$

The Reynolds number is defined in terms of the hydraulic diameter of the parallel plate channel as

$$Re = \frac{4bu_0}{\nu}, \tag{1f}$$

where b is the half-spacing between the plates, u_0 is the uniform velocity at the duct inlet and ν is the kinematic viscosity of the fluid.

The required boundary conditions in terms of the streamfunction are given by

$$\psi(0,\, y) = y, \qquad \frac{\partial \psi(0,\, y)}{\partial x} = 0, \tag{2a, b}$$

$$\psi(\infty,\, y) = \tfrac{3}{2}y - \tfrac{1}{2}y^3, \qquad \frac{\partial \psi(\infty,\, y)}{\partial x} = 0, \tag{2c, d}$$

$$\psi(x,\, 0) = 0, \qquad \frac{\partial^2 \psi(x,\, 0)}{\partial y^2} = 0, \tag{2e, f}$$

$$\psi(x,\, 1) = 1, \qquad \frac{\partial \psi(x,\, 1)}{\partial y} = 0, \tag{2g, h}$$

which represent the inlet conditions ($x = 0$), the fully developed solution ($x \to \infty$), the symmetry condition ($y = 0$) and the no-slip/permeability wall conditions ($y = 1$). The inlet conditions (2a,b) correspond to the more frequently considered situation of a uniform parallel inlet flow ($u = 1, v = 0$). For the second situation analysed here, i.e. the irrotational inlet condition, equations (2a,b) are modified to give

$$\psi(0,\, y) = y, \qquad \frac{\partial^2 \psi(0,\, y)}{\partial x^2} = 0. \tag{2i, j}$$

Following the ideas in the generalized integral transform technique,[8–14] in order to select the appropriate auxiliary eigenvalue problem which will provide a basis for the eigenfunction expansion, the original problem is made homogeneous in the boundary conditions for the co-ordinate selected to be eliminated through integral transformation. Therefore the streamfunction is rewritten as

$$\psi(x,\, y) = \psi^*(x,\, y) + \psi_\infty(y), \tag{3}$$

where $\psi_\infty(y)$ represents the fully developed flow streamfunction. The problem related to $\psi^*(x, y)$ becomes

$$\nabla^4 \psi^*(x,\, y) = \frac{Re}{4} P^*(x,\, y), \quad 0 < y < 1, \quad x > 0, \tag{4a}$$

where

$$P^*(x,\, y) = \left(\frac{\partial \psi^*}{\partial y} + \frac{\mathrm{d}\psi_\infty}{\mathrm{d}y}\right)\left(\frac{\partial^3 \psi^*}{\partial x^3} + \frac{\partial^3 \psi^*}{\partial y^2 \partial x}\right) - \frac{\partial \psi^*}{\partial x}\left(\frac{\partial^3 \psi^*}{\partial x^2 \partial y} + \frac{\partial^3 \psi^*}{\partial y^3} + \frac{\mathrm{d}^3 \psi_\infty}{\mathrm{d}y^3}\right), \tag{4b}$$

with boundary conditions

$$\psi^*(0, y) = \frac{y^3}{2} - \frac{y}{2}, \qquad \frac{\partial \psi^*(0, y)}{\partial x} = 0, \tag{5a,b}$$

$$\psi^*(\infty, y) = 0, \qquad \frac{\partial \psi^*(\infty, y)}{\partial x} = 0, \tag{5c,d}$$

$$\psi^*(x, 0) = 0, \qquad \frac{\partial^2 \psi^*(x, 0)}{\partial y^2} = 0, \tag{5e,f}$$

$$\psi^*(x, 1) = 0, \qquad \frac{\partial \psi^*(x, 1)}{\partial y} = 0. \tag{5g,h}$$

For irrotational inlet flow the conditions (5a,b) are replaced by

$$\psi^*(0, y) = \frac{y^3}{2} - \frac{y}{2}, \qquad \frac{\partial^2 \psi^*(0, y)}{\partial x^2} = 0. \tag{5i,j}$$

For the present biharmonic equation (4a) the appropriate eigenvalue problem is taken as

$$\frac{d^4 Y_i(y)}{dy^4} = \mu_i^4 Y_i(y), \quad i = 1, 2, \ldots, \tag{6a}$$

with boundary conditions

$$Y_i(0) = 0, \qquad \frac{d^2 Y_i(0)}{dy^2} = 0, \tag{6b,c}$$

$$Y_i(1) = 0, \qquad \frac{dY_i(1)}{dy} = 0. \tag{6d,e}$$

The normalized eigenfunctions Y_i have the orthogonality property

$$\int_0^1 Y_i(y) Y_j(y)\, dy = \delta_{ij}, \tag{7}$$

where $\delta_{ij} = 0$ for $i \neq j$ and $\delta_{ij} = 1$ for $i = j$. This allows the definition of the integral transform pair

$$\bar{\psi}_i^*(x) = \int_0^1 Y_i(y) \psi^*(x, y)\, dy, \quad \text{transform}, \tag{8a}$$

$$\psi^*(x, y) = \sum_{i=1}^{\infty} Y_i(y) \bar{\psi}_i^*(x), \quad \text{inversion}, \tag{8b}$$

where $\bar{\psi}_i^*(x)$ represents the integral transformed potential.

Problem (6) can be solved analytically to yield

$$Y_i(y) = \frac{\sin(\mu_i y)}{\sin \mu_i} - \frac{\sinh(\mu_i y)}{\sinh \mu_i}, \quad i = 1, 2, \ldots. \tag{9a}$$

The eigenvalues μ_i are obtained from the transcendental equation

$$\tanh \mu_i = \tan \mu_i, \quad i = 1, 2, \ldots. \tag{9b}$$

The partial differential equation (4a) is now integral transformed through the operator $\int_0^1 Y_i(y)dy$. After evaluation of the individual integrations the transformed system of ordinary differential equations becomes

$$\frac{d^4 \bar{\psi}_i^*}{dx^4} + 2 \sum_{j=1}^{\infty} D_{ij} \frac{d^2 \bar{\psi}_j^*}{dx^2} + \mu_i^4 \bar{\psi}_i^* = \frac{\text{Re}}{4} \bar{P}_i\left(x, \bar{\psi}_j^*, \bar{\psi}_k^*\right), \tag{10a}$$

where

$$D_{ij} = \int_0^1 Y_i(y)\,\frac{d^2Y_j}{dy^2}\,dy \tag{10b}$$

and the transformed source function is given by

$$\begin{aligned}\bar{P}_i\left(x,\,\bar{\psi}_j^*,\,\bar{\psi}_k^*\right) = -\sum_{j=1}^{\infty}\Bigg[\sum_{k=1}^{\infty}\left(A_{ijk}\frac{d\bar{\psi}_j^*}{dx}\bar{\psi}_k^* + B_{ijk}\frac{d\bar{\psi}_j^*}{dx^2}\frac{d^2\bar{\psi}_k^*}{dx^3} - C_{ijk}\bar{\psi}_j^*\frac{d\bar{\psi}_k^*}{dx} - B_{ijk}\bar{\psi}_k^*\frac{d^3\bar{\psi}_j^*}{dx^3}\right)\\ - B_{\infty ij}\frac{d^3\bar{\psi}_j^*}{dx^3} - \left(A_{\infty ij} - C_{\infty ij}\right)\frac{d\bar{\psi}_j^*}{dx}\Bigg],\end{aligned} \tag{11a}$$

with

$$A_{ijk} = \int_0^1 Y_iY_j\frac{d^3Y_k}{dy^3}\,dy, \qquad B_{ijk} = \int_0^1 Y_iY_j\frac{dY_k}{dy}\,dy, \tag{11b,c}$$

$$C_{ijk} = \int_0^1 Y_i\frac{dY_j}{dy}\frac{d^2Y_k}{dy^2}\,dy, \qquad C_{\infty ij} = \int_0^1 Y_iY_j\frac{d^3\psi_\infty}{dy^3}\,dy, \tag{11d,e}$$

$$A_{\infty ij} = \int_0^1 Y_iY_j\frac{d\psi_\infty}{dy}\,dy, \qquad B_{\infty ij} = \int_0^1 Y_i\frac{d^2Y_j}{dy^2}\frac{d\psi_\infty}{dy}\,dy. \tag{11f,g}$$

The boundary conditions in the x-co-ordinate, required for the solution of system (10), are also integral transformed accordingly to yield

$$\bar{\psi}_i^*(0) = \tfrac{1}{2}\int_0^1 (y^3 - y)Y_i(y)\,dy, \qquad \frac{d\bar{\psi}_i^*(0)}{dx} = 0, \tag{12a,b}$$

$$\bar{\psi}_i^*(\infty) = 0, \qquad \frac{d\bar{\psi}_i^*(\infty)}{dx} = 0. \tag{12c,d}$$

Again, for irrotational inlet flow equation (12b) becomes

$$\frac{d^2\bar{\psi}_i^*(0)}{dx^2} = 0. \tag{12e}$$

Once the transformed potentials $\bar{\psi}_i^*(x)$ have been numerically computed along the x-direction through the appropriate algorithm for boundary value problems, as discussed in the next section, the inversion formula (8b) is recalled to provide the streamfunction explicitly at any prescribed position in the y-direction.

COMPUTATIONAL PROCEDURE

The computational algorithm can be readily constructed, including the desirable features of automatically controlling the global error in the final solution for the streamfunction at selected points and of avoiding the need for approximating the outflow boundary condition at an arbitrary finite duct length.

Therefore the truncated version of boundary value problem (10–12) to any specified finite order N is numerically handled, for instance, through subroutine DBVPFD from the IMSL library,[15] which offers an automatic adaptive scheme for local error control of the transformed potentials results. Before utilizing this routine, the system (10–12) is rewritten as a first-order ODE system of $4N$ equations. Also, the original fully developed flow boundary conditions at $x \to \infty$, equations (12c,d), are exactly satisfied through an algebraic transformation of the independent variable x, which is mapped into the finite domain $0 \leq \eta \leq 1$. Possible choices for such a transformation are given by

$$\eta = 1 - (1 + cx)^{-1}, \tag{13a}$$

$$\eta = 1 - e^{-cx}, \tag{13b}$$

where c is a positive constant which may be varied according to the Reynolds number considered to accelerate convergence. Since we are dealing with ordinary differential equations only, the transformation becomes quite straightforward. Besides, these numerical results allow for a critical inspection of the effects on the final converged solution when one truncates the duct to a finite length L and imposes fully developed conditions at the duct end.

Since all the intermediate numerical tasks are accomplished within a prescribed accuracy, one is left with the job of reaching convergence in the eigenfunction expansions and automatically controlling the truncation order N for the requested number of fully converged digits in the final solution for the streamfunction at those positions of interest.

The analytic form of the inverse formula (8b) allows for a direct testing procedure at each specified position within the medium, and the truncation order N can be gradually increased in fixed steps $N + \Delta N$ until convergence is reached at all desired locations. In addition, the numerical results already available for the lower-order N serve as an excellent initial guess for the iterative procedure implemented within the boundary value problem solver, providing a marked reduction in computational cost. The simple tolerance-testing formula

$$\epsilon = \max_{(x,y)} \left| \frac{\sum_{i=N+1}^{N+\Delta N} Y_i(y)\bar{\psi}_i^*(x)}{\sum_{i=1}^{N+\Delta N} Y_i(y)\bar{\psi}_i^*(x) + \psi_\infty(y)} \right| \tag{14}$$

is employed until ε satisfies the required global error over all the positions (x, y) requested. Once the transformed streamfunctions are available, the velocity components $u(x, y)$ and $v(x, y)$ are directly evaluated from their definitions, equations (1b,c), after substitution of the inversion formula (8b), to yield

$$u(x, y) = \sum_{i=1}^{N} \frac{dY_i(y)}{dy}\bar{\psi}_i^*(x) + U_\infty(y), \qquad v(x, y) = -\sum_{i=1}^{N} Y_i(y)\frac{d\bar{\psi}_i^*(x)}{dx}, \tag{15a, b}$$

where

$$U_\infty(y) = \tfrac{3}{2}(1 - y^2). \tag{15c}$$

However, it is a well-known fact in eigenfunction expansion approaches [8] that the series formed from derivatives of the eigenfunctions may experience a slow convergence, since the monotonically increasing eigenvalues appear in the numerator of the infinite summations. This behaviour was again illustrated for the case of a lid-driven cavity flow in Reference 10. Therefore the axial velocity component $u(x, y)$ is alternatively evaluated from an error-controlled numerical differentiation of the fully converged results for the streamfunction. The routine DERIV from the IMSL library[15] is easily implemented for this purpose and equation (15a) is then avoided.

RESULTS AND DISCUSSION

First of all the algorithm is employed to yield benchmark results for the special case of creeping flow ($Re = 0$), which is also used to validate the automatic global error control scheme. A relative error target of 10^{-4} is selected and convergence is considered to be attained to within $\pm$ 1 in the fourth digit of the streamfunction. Table I illustrates the convergence behaviour of the duct centreline longitudinal velocity $u(x, 0)$ at various axial positions for increasing truncation order in the streamfunction eigenfunction expansions. The velocity component is converged to four digits at quite low expansion orders ($N \simeq 5$–7). As expected in eigenfunction-expansion-type approaches, the convergence is improved away from the duct inlet.

Table II presents the same convergence behaviour of the longitudinal velocity component but for the case $Re = 40$, which has been previously studied through purely numerical approaches (finite difference[2] and finite element[6] methods). Essentially the same convergence behaviour is observed in comparison with the previous case of $Re = 0$, and the fully converged results validate the computations in References 2 and 6, with a reasonably good agreement to three digits in both cases and a slightly better confirmation of the results of the finite difference approach of Reference 2.

A higher Reynolds number ($Re = 300$) was also considered, including the effect of the inlet flow condition. The overall convergence behaviour is not markedly affected by the increased importance of the convective terms, as seen in Table III but a few extra terms were required to achieve convergence in the position closest to the duct inlet ($x = 0{\cdot}20833$) in comparison with the previous cases of lower values of Re. The finite difference results presented in graphical form in Reference 5 are in good agreement with the error-controlled integral transform computations. The irrotational inlet flow condition also demonstrates a slight influence on convergence rates. The more recent numerical implementation of Reference 5 achieves a better agreement, to three digits, with the present fully converged results than the early work of Wang and Longwell.

The influence of prescribing the outflow fully developed boundary condition on a finite duct length was also investigated. Table IV shows the longitudinal velocity component at various axial positions along the channel, with $Re = 40$ and 300, for increasing truncated duct lengths L, as well as the reference results for an infinite duct. It can be noticed that results in the region close to the duct inlet are not affected by the artificial boundary condition imposed on the finite lengths selected. As the duct length is reduced ($L = 2$) and the computations are performed for increasing axial positions, the outflow boundary condition imposed starts perturbing the velocity field behaviour upstream quite significantly. Therefore a reliable implementation of a purely numerical approach must include an investigation of the appropriate value of L for each Reynolds number, since L should be increased with Re, thus increasing the overall computational effort. On the other hand, the use of a conservatively large value of L would bring the need for further mesh refinement and, again, increased computational cost. The present hybrid numerical–analytical approach completely avoids such difficulties and adds the quite desirable feature of automatic error control and estimation. Figure 2 presents an interesting comparison of fully converged integral transform results from both the present Navier–Stokes

Table I. Convergence behaviour of the duct centreline longitudinal velocity component, $u(x,0)$, for $Re = 0$ (inlet conditions: $u = 1$, $v = 0$)

N	$x = 0{\cdot}2$	$x = 0{\cdot}4$	$x = 0{\cdot}6$	$x = 0{\cdot}8$
3	1·031	1·193	1·319	1·405
5	1·058	1·198	1·320	1·405
7	1·065	1·198	1·321	1·406
9	1·066	1·198	1·321	1·406
11	1·066	1·198	1·321	1·406
13	1·066	1·198	1·321	1·406

Table II. Convergence behaviour of the duct centreline longitudinal velocity component, $u(x, 0)$, for $Re = 40$, and comparison with purely numerical solutions (inlet conditions: $u = 1$, $v = 0$)

N	$x = 0{\cdot}2$	$x = 0{\cdot}4$	$x = 0{\cdot}6$	$x = 0{\cdot}8$
3	0·9772	1·075	1·162	1·246
5	1·012	1·083	1·165	1·250
7	1·020	1·083	1·166	1·251
9	1·022	1·083	1·166	1·251
11	1·022	1·083	1·166	1·251
13	1·022	1·083	1·166	1·251
Ref. [2]	1·0223	1·0849	1·1693	1·2535
Ref. [7]	1·0243	1·0884	1·1737	1·2580

Table IIIa. Convergence behaviour of the duct centreline longitudinal velocity component, $u(x,0)$, for $Re = 300$ (inlet conditions: $u = 1$, $v = 0$)

N	$x = 0{\cdot}20833$	$x = 0{\cdot}8333$	$x = 3{\cdot}3333$	$x = 7{\cdot}5$
3	0·9178	1·054	1·273	1·423
5	0·9740	1·072	1·279	1·425
7	0·9976	1·071	1·280	1·425
9	1·006	1·071	1·280	1·425
11	1·008	1·071	1·280	1·425
13	1·007	1·071	1·280	1·425
15	1·007	1·071	1·280	1·425
17	1·007	1·071	1·280	1·425
Ref.[5]	1·008	1·075	1·283	1·425

Table IIIb. Convergence behaviour of the duct centreline longitudinal velocity component, $u(x,0)$, for $Re = 300$ (inlet conditions: $u = 1$, $\omega = 0$)

N	$x = 0{\cdot}20833$	$x = 0{\cdot}8333$	$x = 3{\cdot}3333$	$x = 7{\cdot}5$
5	1·022	1·134	1·316	1·437
7	1·041	1·145	1·324	1·440
9	1·047	1·153	1·328	1·441
11	1·048	1·159	1·331	1·442
13	1·049	1·163	1·333	1·443
15	1·050	1·166	1·335	1·443
17	1·051	1·168	1·336	1·444
19	1·052	1·170	1·337	1·444
Ref.[1]	1·0581	1·1880	1·3572	1·4509
Ref.[5]	1·050	1·170	1·34	1·44

Table IVa. Influence of boundary condition for a truncated duct length on centreline longitudinal velocity component, $u(x, 0)$ with $Re = 40$ (inlet conditions: $u = 1$, $v = 0$)

x	$L = 2$	$L = 4$	$L = 6$	$L = \infty$
0·2	1·022	1·022	1·022	1·022
0·6	1·166	1·166	1·166	1·166
1·0	1·323	1·322	1·322	1·322
1·4	1·421	1·417	1·417	1·417
1·8	1·480	1·463	1·463	1·463
2·0	1·5	1·475	1·475	1·475

Table IVb. Influence of boundary condition for a truncated duct length on centreline longitudinal velocity component, $u(x,0)$, with $Re = 300$ (inlet conditions: $u = 1$, $v = 0$)

x	$L = 8$	$L = 10$	$L = 15$	$L = \infty$
0·20833	1·007	1·007	1·007	1·007
0·8333	1·071	1·071	1·071	1·071
3·3333	1·280	1·280	1·280	1·280
7·5	1·437	1·425	1·425	1·425

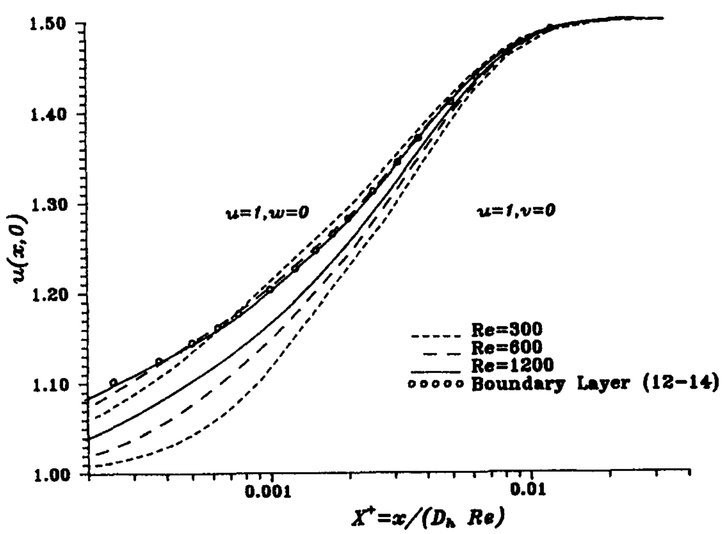

Figure 2. Comparison of centreline longitudinal velocity evolution along duct length between Navier–Stokes and boundary layer formulations

formulation, with various types of inlet conditions, and the classical boundary layer approximation. The centreline longitudinal velocity component is plotted against a dimensionless axial co-ordinate containing the Reynolds number, which collapses the boundary layer results into one single curve. Clearly the numerical results following the irrotational inlet flow condition ($u = 1$, $\omega = 0$) are much closer to the boundary layer results in the vicinity of the duct inlet for all three values of the Reynolds number considered. On the other hand, the results from the uniform parallel inlet condition($u = 1$, $v = 0$) tend more slowly to the approximate boundary layer solution for increasing values of Re. Therefore the appropriateness of the boundary layer approximation for a specific flow situation and Re-value is closely connected to the proper identification of the actual flow inlet condition, and a simple criterion based on the magnitude of Re might not be safe enough for accurate evaluation of a developing flow situation.

Figure 3 shows a comparison of the longitudinal velocity profiles along the developing region, as obtained from both inlet flow conditions, for $Re = 300$. The expected central concavity of the longitudinal velocity distribution is more clearly observable in the situation of uniform parallel inlet flow, while the irrotational flow inlet results are more closely behaved to the boundary layer solution. The influence of the inlet flow situation is practically unnoticeable for regions a little away from the duct inlet region, as represented by the results at $x = 3{\cdot}333$ and $7{\cdot}5$. Finally, Figure 4 illustrates the development of the transverse velocity component along the duct entry region, showing the expected migration of the relative maximum towards the duct centreline as the flow develops.

The computer code was implemented on a VAX8810 mainframe computer and typical CPU times can be reported for $Re = 40$ ($\simeq$160 s) and $Re = 300$ ($\simeq$15 min). It should be noted that these CPU time values correspond to fully converged results to four significant digits at various positions within the channel, as achieved through the automatic error procedure, all in a single run. For further improvement in convergence rates and consequently computational cost reduction, the filtering technique can be employed additional times at the cost of increased analytical involvement.

The extension of this approach to different classical test cases should now proceed in an attempt to establish sets of benchmark results for reference purposes by users of the various numerical techniques. Therefore the present effort should now be continued into the analysis of transient formulations, complex geometries and turbulent regimes, following the previous contributions on diffusion problems and boundary layer equations.[8]

Although this same problem could have been handled through the primitive variables formulation, it has been demonstrated in previous developments[9–14] that the choice of the eigenvalue problem inherent to the streamfunction-only formulation provides improved convergence behaviour over the primitive variables choice.

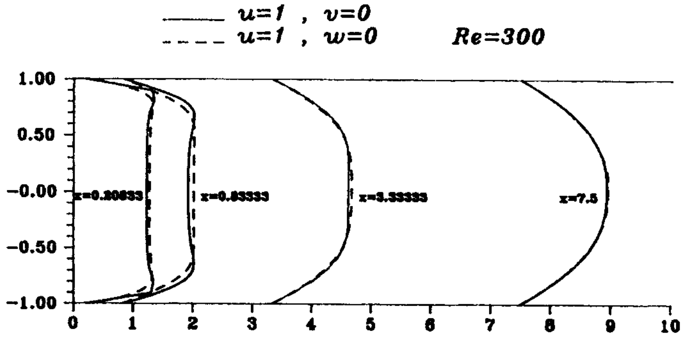

Figure 3. Development of longitudinal velocity profile along duct length for both uniform/parallel and irrotational inlet conditions (Re = 300)

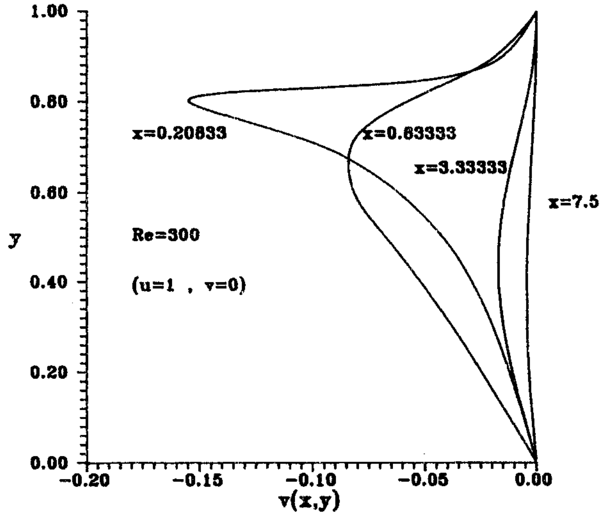

Figure 4. Development of transverse velocity profile along duct length (Re = 300; inlet conditions: u = 1, v = 0)

ACKNOWLEDGEMENTS

The authors wish to acknowledge the partial financial support provided by the British Council in Rio de Janeiro, Brazil through the research link with the Institute for Numerical Methods in Engineering, University College of Swansea, U.K.

REFERENCES

1. Y. L. Wang and P. A. Longwell, 'Laminar flow in the inlet section of parallel plates', *AICHE J.*, **10**, 323–329(1964).
2. A. Brandt and J. Gillis, 'Magnetohydrodynamic flow in the inlet region of a straight channel', *Phys Fluids*, **9**, 690–699(1966).
3. S. Abarbanel, S. Bennet, S. Brandt and J. Gillis, 'Velocity profiles of flow at low Reynolds numbers', *J.Appl.Mech.*, 2–4(1970).
4. H. Morihara and R. T. Cheng, 'Numerical solution of viscous flow in the entrance region of parallel plates', *J.Comp.Phys.*, **11**, 500–572(1973).
5. J. W. McDonald, V. E. Denny and A. F. Mills, 'Numerical solutions of the Navier–Stokes equations in inlet regions', *J.Appl.Mech.*, **39**, 873–878(1972).
6. B. S. Narang and G. Krishnamoorthy, 'Laminar flow in the entrance region of parallel plates', *J.Appl.Mech.*, **43**, 186–188(1976).
7. G. Comini and S. Del Giudice, 'Finite element solution of the incompressible Navier–Stokes equations', *Num. Heat Transfer*, **5**, 463–478(1982).
8. R. M. Cotta, *Integral transforms in computational heat and fluid flow*, CRC Press, Boca Raton, FL, 1993.
9. J. S. Perez Guerrero and R. M. Cotta, 'Integral transform solution for the lid-driven cavity flow problem in streamfunction-only formulation', *Int.J.Numer.Methods Fluids*, **15**, 399–409(1992).
10. R. M. Cotta, J. S. Perez Guerrero and F. Scofano Neto, 'Hybrid solution of the incompressible Navier–Stokes equations via integral transformation'. In, *Proc. 2nd Int.Conf. on Advanced Computational Methods in Heat Transfer*, **1**, 735–750, Milan, Italy, 1992.
11. C. Baohua and R. M. Cotta, 'Integral transform analysis of natural convection in porous enclosures', *Int. J. Numer. Methods Fluids*,**17**, 787–801(1993).
12. R. M. Cotta and T. M. B. Carvalho, 'Hybrid analysis of boundary layer equations for internal flow problems'. In, *Proc. 7th Int.Conf. on Num.Meth. in Laminar and Turbulent Flow*, **1**, 106–115, Stanford, CA, 1991.
13. T. M. B. Carvalho, R. M. Cotta and M. D. Mikhailov, 'Flow development in the entrance region of ducts', *Comm. Numer. Methods. Engng.*, **9**, 503–509(1993).
14. H. A. Machado and R. M. Cotta, 'Integral transform method for boundary layer equations in simultaneous heat and fluid flow problems', *Int. J. Num. Meth. Heat Fluid Flow*, in press.
15. IMSL Library, MATH/LIB, Houston, Texas, 1989.